Prediction of enteric methane emission from beef cattle in Southeast Asia

Improving national greenhouse gas (GHG) inventories is important in projecting GHG emission trends and constructing mitigation strategies. The significant contributions of enteric methane (CH_4) emissions to global GHG emissions indicate the necessity for improving CH_4 emission estimates. Enteric CH_4 from ruminants is produced during fermentation of dietary carbohydrates in the rumen, and consequently, enteric CH_4 emission is principally affected by feed intake and the type and digestibility of feed. Therefore, various equations based on dietary intake and its components for estimating enteric CH_4 emission have been provided for animal species, production systems, and regions. However, little information is available in Southeast Asia, a region characterized by producing large numbers of beef cattle in monsoonal agricultural systems focused on rice production. To develop equations for estimating enteric CH_4 emissions from beef cattle in Southeast Asia using commonly available indices, we carried out meta-data analysis using data obtained in Thailand and Vietnam.

During the period 2005–2015, individual data (n = 332) were collected from 25 studies carried out in Thailand and Vietnam using a ventilated respiration apparatus equipped with a head hood. The dataset included observations on feed chemical composition, nutrient intakes, digestibilities, and CH_4 emissions. The animals from which data were obtained were Brahman male cattle (n = 171), Thai native male cattle (n = 121), and Lai Sind male cattle (n = 40; Photo 1).

The best equation to predict daily CH_4 emissions included dry matter intake and ether extract contents (Equation 1 in Table 1). The equation including only dry matter intake as a variable was also good for prediction (Equation 2). The best equation to predict methane conversion factor, expressed as CH_4 energy as a portion of gross energy intake, was obtained using DMI per body weight, content of ether extract and crude protein, and DM digestibility (Equation 3). Mean methane conversion factor (MCF) of cattle in High roughage group (≥0.68 kg/kg in their feed as DM) was higher than that of cattle in Medium (0.34–0.67 kg/kg) and Low (≤0.33 kg/kg) roughage groups (8.1%, 7.3% and 7.3%, respectively; Figure 1). Those MCFs were higher than default MCF by the Intergovernmental Panel on Climate Change (IPCC; 6.5 ± 1.0%) for cattle, excluding fattening cattle fed diets containing 90% or more concentrates. These higher MCFs were considered to reflect the characteristics of cattle feed containing relatively higher fiber contents in Southeast Asia. These present equations are applicable to improving CH_4 emission estimation in Southeast Asia.

(T. Suzuki [NARO Institute of Livestock and Grassland Science], K. Sommart [Khon Kaen University, Thailand], W. Angthong [Ruminants Feeding Standard Research and Development Center, Thailand], V. T. Nguyen [Can Tho University, Vietnam], A. Chaolaur [Silpakorn University, Thailand], P. Nitipot [Kalasin University, Thailand], Y. Cai [NARO Institute of Livestock and Grassland Science], T. Nishida [Obihiro University of Agriculture and Veterinary Medicine], F. Terada [Tohoku University], T. Sakai [University of Miyazaki], T. Kawashima [University of Miyazaki])

Photo 1. Cattle breeds used in measuring methane emissions

Table 1. Regression equations for predicting daily methane emission and methane energy as a proportion of gross energy intake in cattle

	RMSE	R^2
(1) CH_4 = 22.67×DMI − 3.73×EE + 23.32	18.64	0.783
(2) CH_4 = 22.71×DMI + 8.91	19.36	0.766
(3) MCF = −0.782×DMIBW − 0.436×EE−0.073×CP + 0.049×DMD + 8.654	1.348	0.391

CH_4, daily methane emission (g/day); MCF, methane conversion factor expressed as methane energy as a portion of gross energy intake (J/100 J); DMI, dry matter (DM) intake (kg/day); EE, ether extract content (% DM); CP, crude protein content (% DM); NDF, content of neutral detergent fiber (% DM); DMD, DM digestibility (%); DMIBW, DMI per BW (kg/100 kg); RMSE, root mean square error.

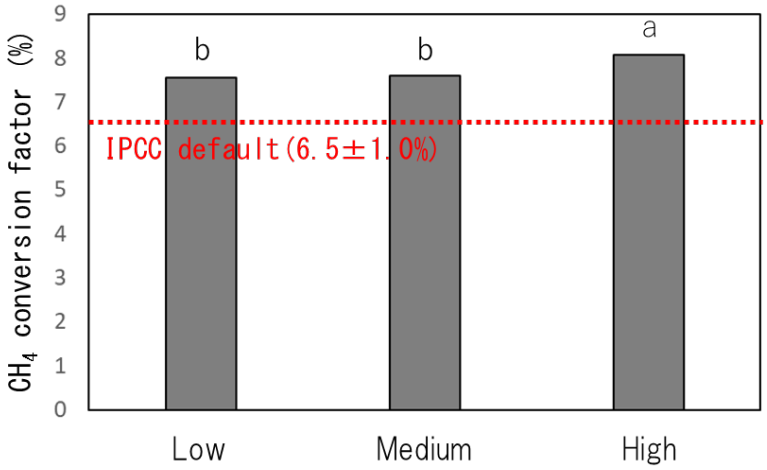

Fig. 1. Methane conversion factors in cattle by roughage proportion groups. Cattle were separated by roughage proportion (DM basis) into Low roughage (≤0.33 kg/kg), Medium roughage (0.34–0.67 kg/kg), and High roughage (≥0.68 kg/kg) groups. Dashed line shows default methane conversion factor for cattle excluding feedlot fed cattle.
$^{ab}P<0.05$

Cassava pulp is suitable as beef cattle feed and shows less variation in chemical contents among seasons and factories

Cassava (*Manihot esculenta*) is one of Thailand's major crops, with about half of domestic production coming from the northeastern region. Cassava pulp, the major waste produced from starch factories, is considered a nutritious feed for cattle because of its high starch and fiber contents. To promote cassava pulp utilization as cattle feed, variations in chemical composition among seasons and starch factories, energy value, and performance of beef cattle fed with cassava pulp were investigated.

Cassava pulp samples were collected in each season -- the rainy season (mid-May to mid-October), summer (mid-October to mid-February), and winter (mid-February to mid-May) -- from four starch factories in northeastern Thailand. Significant variations in phosphorus and potassium contents were found among factories (Table 1). Constant variation in any of the chemical components was not found among the three seasons. Crude protein content of cassava pulp was close to that of cassava chip. Energy values, obtained from feeding trial using four Thai native cattle fed basal diet or basal diet with cassava pulp at maintenance level, were close to that of dried brewers' grain.

Eighteen yearling Thai native cattle were allocated to one of three dietary treatments and fed ad libitum (i.e., as much as desired) for 5 months in a randomized complete block design. Three dietary treatments using different proportions of cassava pulp (10, 30 and 50% as dry matter) instead of rice straw as a base in a fermented total mixed ration were applied (Table 2). The diets were formulated to contain 10% crude protein and exceed their energy requirement. Metabolized energy content and daily weight gain increased with increasing cassava pulp content (Fig. 1).

These results provide useful information on beef cattle rearing using cassava pulp and contribute in promoting the utilization of waste (cassava pulp) from cassava factories. Cassava pulp should be used as soon as possible or kept under anaerobic condition because of its low aerobic stability. The physical effective fiber content and nutrient requirements must be noted when diets are formulated with a high cassava pulp ratio.

T. Suzuki [NARO Institute of Livestock and Grassland Science], O. Kaeokliang [Ruminants Feeding Standard Research and Development Center, Thailand], W. Angthong [Ruminants Feeding Standard Research and Development Center, Thailand], R. Narmseelee [Ruminants Feeding Standard Research and Development Center, Thailand], T. Kawashima [University of Miyazaki], K. Kongphitee [Khon Kaen University, Thailand], T. Gunha [Khon Kaen University, Thailand], K. Sommart [Khon Kaen University, Thailand], T. Phonbumrung [Bureau of Animal Nutrition Development, Department of Livestock Development, Thailand])

Table 1. Chemical composition and energy values of cassava pulp, cassava chip and dried brewers' grain

	Cassava pulp		Cassava chip§	Dried brewers' grain§
	Mean	SD		
DM (%)	18.4	3.9	89.8	91.3
Crude Protein (%DM)	2.2	0.5	2.3	25
Ether extract (%DM)	0.4	0.3	0.5	5.7
Neutral detergent fiber (%DM)	36.0‡	5.1	10.1	50.7
Non fibrous carbohydrate (%DM)	59.3‡	5.4	10.8	83.3
Hydrocyanic acid (ppm DM)	117	55	–	–
Calcium (%DM)	0.22	0.07	0.1	0.36
Phosphorus (%DM)	0.03†	0.01	0.1	0.47
Potassium (%DM)	0.36†	0.14	0.92	0.04
Magnesium (%DM)	0.09	0.02	0.09	0.23
Total digestible nutrient (%DM)	74.4	0.4	79	70
Metabolized energy (MJ/kgDM)	11.3	0.1	15.3	11.3

DM:dry matter, †significant difference among factories (P<0.05)、‡interaction between factory and season (P<0.05), §Data obtained from Nutrient Requirements of Beef Cattle in Indochinese Peninsula (2010)

Table 2. Feed formula, chemical composition and energy value of fermented total mixed ration containing 10, 30 and 50% of cassava pulp (dry matter basis)

	Cassava pulp ratio		
	Low	Medium	High
Feed formula (DM basis)			
Cassava pulp	**10.0**	**30.0**	**50.0**
Rice straw	50.0	30.0	10.0
Palm Kernel meal	23.5	23.5	23.5
Soybean meal	5.0	5.0	5.0
Rice bran	10.0	10.0	10.0
Urea	0.5	0.5	0.5
Vitamin & mineral premix	1.0	1.0	1.0
Chemical composition (%DM)			
Crude protein	9.9	9.7	9.7
Ether extract	5.9	5.9	5.9
Neutral detergent fiber	63.2	53.6	45.2
Non fibrous carohydrate	10.5	22.9	33.7
Metabolized energy (MJ/kgDM)	**9.6**	**11.4**	**12.4**

DM: dry matter

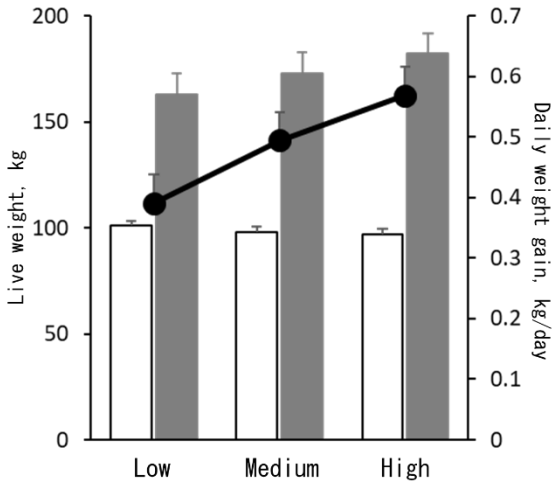

Fig. 1. Initial (□) and final (■) live weight, and daily weight gain (●) of Thai native cattle fed fermented total mixed ration containing 10, 30 and 50% of cassava pulp (dry matter basis; Low, Medium, and High, respectively). Daily weight gain linearly increased with increasing cassava pulp inclusion (P<0.05).

Improvement of rice grain yield by predicting the optimum sowing period for rainfed rice areas in the Asian monsoon region

Unlike irrigated rice fields, rainfed rice areas in the Asian monsoon region depend mainly on rainfall for water supply, bringing down rice productivity to nearly half of those in irrigated areas. Despite this fact, rainfed rice areas play a crucial role in meeting future demand for the staple food; thus, it is imperative that high and stable productivity is achieved through appropriate technology development. Rainfall pattern changes year to year and rainfed rice farmers can hardly anticipate the optimum sowing period for better grain yield. Seasonal climate prediction is relevant for the current problems in rainfed areas, and the expected technology for predicting rice grain yield will be applied and developed through ORYZA, a crop growth modelling tool. SINTEX-F, the coupled ocean-atmosphere general circulation model developed by the Japan Agency for Marine-Earth Science and Technology (JAMSTEC), has a few months to one-year lead time predictability and is used for grain yield prediction through ORYZA, which in turn requires daily weather data to obtain grain yield as a function of sowing timings.

SINTEX-F is designed for predicting the El Niño-Southern Oscillation (ENSO), which has a high correlation to the Asian monsoon. However, SINTEX-F has a bias, hence it cannot be directly used for ORYZA. Thus, the outputs need to be corrected through statistical downscaling within 100 km^2. The results through statistical downscaling of SINTEX-F outputs show a high correlation with locally observed weather data (Fig. 1). On the other hand, model fit of ORYZA for grain yield simulation is excellent even for different sowing timings (Fig. 2). With these obtained results, grain yields can be predicted through hindcast analysis of ORYZA with downscaled predictions as it demonstrates a high correlation with grain yields obtained with observed weather data (Fig. 3).

When Ciherang, one of the most popular rice varieties in Indonesia, was grown with the recommended fertilizer application in Central Java, the grain yield by farmers who based their sowing timing on predictions was higher than those who missed the optimum timing because they did not rely on predictions (Fig. 4). The improvement in grain yield for the first group of farmers was significant when compared to the area's average grain yield, which was 3.42 t ha^{-1} (Boling et al. 2008).

The obtained results can be applied to improve the predictability of WeRise, a decision support system for rainfed rice areas and another decision support system for rice that is operated in Indonesia. However, the improvement in grain yield should be combined with appropriate fertilizer management in addition to optimum sowing timings. SINTEX-F predictions should be updated once a year and this entails a cost of 60,000 JPY/100 km^2. Other sources for seasonal climate predictions should be scouted in target countries in Southeast Asia for sustainable operation of the developed technology. In addition, a crop, soil, and local weather database must be developed as it is a prerequisite for ORYZA operation.

(K. Hayashi, L. Llorca [IRRI], R. Agbisit [IRRI], I. Bugayong [IRRI], T. Ishimaru [NARO])

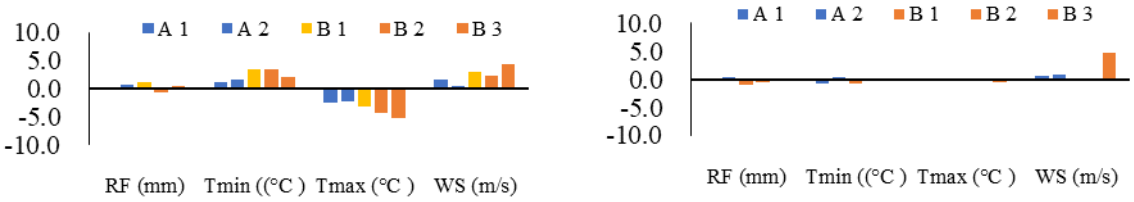

(a) Mean errors between observed weather and SINTEX-F predictions before statistical downscaling

(b) Mean errors between observed weather and SINTEX-F predictions after statistical downscaling

Fig. 1. Statistical downscaling for bias correction of SINTEX-F predictions.
A1, A2: Sites in the Philippines; B1, B2, B3: Sites in Indonesia

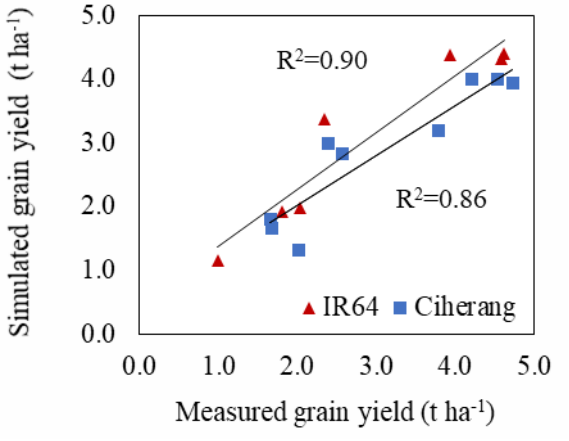

Fig. 2. Accuracy of ORYZA for predicting grain yields at different sowing dates
Red triangle: IR64, Blue square: Ciherang, each point represents its sowing date

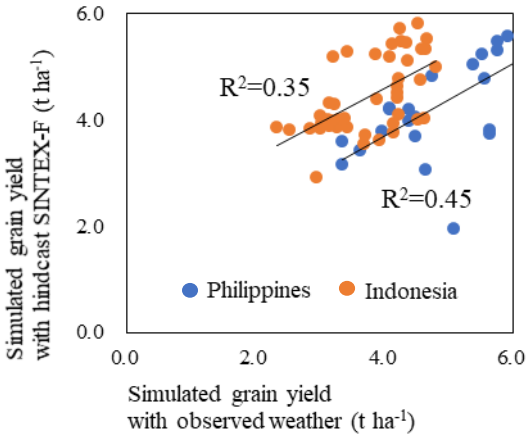

Fig. 3. Grain yield predictability through statistically downscaled SINTEX-F in ORYZA

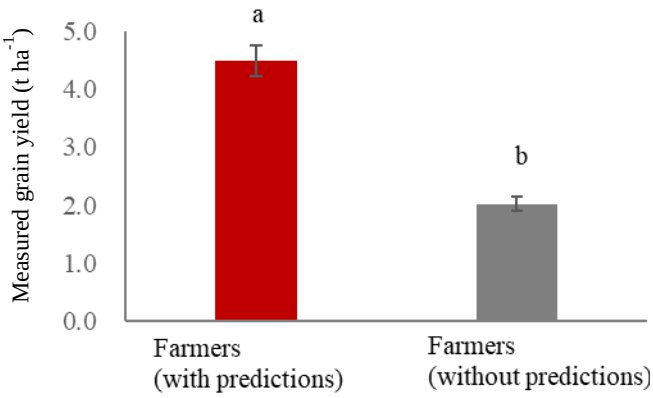

Fig. 4. Improvement in farmers' grain yield with predictions for optimum sowing timing.
Bars in the graph show measured grain yield for the group of farmers with predictions for optimum sowing period and others without predictions. Five farmers were selected randomly for each group. Farmers with predictions were instructed for sowing period (from November 6 to December 10) and variety, while farmers without predictions were instructed only for variety. Sowing period for farmers without predictions was from October 10 to October 25. Different alphabets in the graph mean significant differences at 5% level by Tukey's test.

Ground-penetrating radar can predict the soil depth at which the petroplinthic horizon starts in the Sudan Savanna, West Africa

In the Sudan Savanna (annual rainfall: 600–900 mm), Plinthosols having a petroplinthic (PP) horizon are widely distributed. Because the PP horizon reduces soil volume and storage of water and nutrients, crop production in areas occupied by Plinthosols becomes limited. However, the distribution of Plinthosols has not been precisely known and conventional soil surveys require too much cost and effort. Therefore, at the Institute of Environment and Agricultural Research (INERA) Saria Station, Burkina Faso, we examined if ground-penetrating radar (GPR) can predict the soil depth at which the PP horizon starts or the top boundary of the PP horizon (*d* in Fig. 1). GPR is an equipment that can be used to detect soil interfaces that have abrupt boundaries and contrasting soil materials. In this study, effective soil depth is defined as the soil depth at which the PP horizon starts (*d* in Fig. 1) since only the soils overlying the PP horizon would contribute to crop production.

Our findings are as follows:

- Because relative permittivity of the PP horizon (ε_2 in Fig. 1) is much higher than that of the overlying horizon (ε_1 in Fig. 1), GPR can predict the top boundary of the PP horizon (Figs. 1 and 2).
- Dominant soils in the Sudan Savanna (i.e., Ferric Lixisols, Petric Plinthosols and Pisoplinthic Petric Plinthosols) can be distinguished from the top boundary of the PP horizon (Ikazaki et al., 2018), and sorghum yield positively correlated with effective soil depth (Fig. 3). Therefore, maps of soil types and soil productivity can be easily created by using GPR (without conventional surveys).
- The top boundary of the PP horizon can be determined from a scanned image through a simple correction, enabling the procedure for making maps of soil types and soil productivity to become user friendly.
- Note that the above procedure can be applied only where the soil becomes very dry. This is because soil water having higher permittivity than PP horizons prevents GPR from detecting the top boundary of the PP horizon. This procedure may be applied to dry areas of Brazil and East Africa where PP horizons are widely observed.

With these findings, researchers studying soil and water conservation, fertilization methods, crop breeding, and so forth would be able to take greater account of the inherent soil conditions, which in turn would accelerate their studies for achieving sustainable agriculture in the Sudan Savanna.

(K. Ikazaki, F. Nagumo, S. Simporé [Institute of the Environment and Agricultural Research, Burkina Faso], A. Barro [Institute of Environment and Agricultural Research, Burkina Faso])

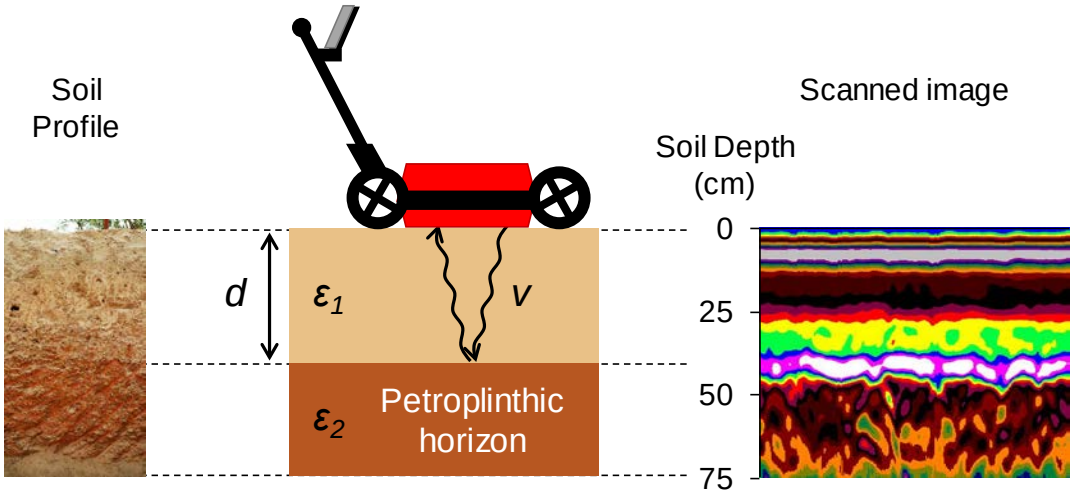

Fig. 1. Schematic diagram of the detection of the petroplinthic horizon

The soil depth at which the petroplinthic horizon starts (*d*) can be estimated by converting the time it took the radar to travel from the surface to the boundary, assuming that the electromagnetic wave velocity in a vacuum is 3.0×10^8 m sec^{-1} and ε_1 was 3.0.

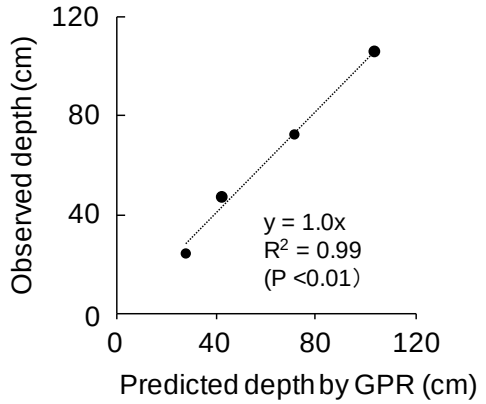

Fig. 2. Relationship between predicted depth and observed soil depth at which the petroplinthic horizon starts (*d* in Fig. 1)

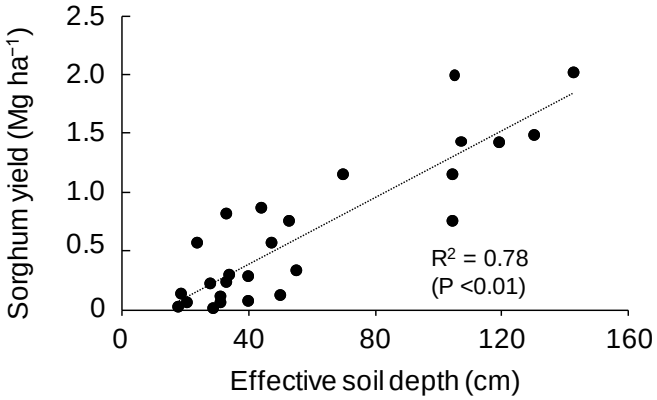

Fig. 3. Relationship between sorghum yield and effective soil depth (*d* in Fig. 1)

Figs. 2 and 3 are cited from Ikazaki et al. 2018. Soil Science and Plant Nutrition, 64(5), 623-631. doi:10.1080/00380768.2018.1502604

Conservation agriculture without intercropping component can adequately control water erosion in the Sudan Savanna, West Africa

In the Sudan Savanna (annual rainfall: 600–900 mm), soil erosion caused by water is severe and a major threat to sustainable agriculture because it depletes soil nutrient and productivity. Conservation agriculture (CA) recommended by the FAO consists of three components: minimum soil disturbance, soil cover, and crop rotation/association. CA was expected to become an effective countermeasure against water erosion in the Sudan Savanna but it has not been adopted by local smallholder farmers because the three-component CA package is considered a heavy burden by farmers who have meager cash and labor resources. Therefore, we examined whether legume intercropping as a crop rotation/association component is vitally necessary for preventing water erosion in the Sudan Savanna.

Three-year field experiments were conducted in runoff plots at the Institute of the Environment and Agricultural Research (INERA) Saria Station, Burkina Faso, and the following findings were obtained:

- Reduced soil loss in both three-component CA package and CA without intercropping was mainly attributed to the reduction in the runoff coefficient (not in the sediment concentration) (Fig. 1).
- CA without intercropping, i.e., with minimum tillage (MT) and sorghum residue mulching (SRM), effectively reduced the annual soil loss by 54% mainly due to the improvement of soil permeability by the boring of termites and wolf spiders found under the sorghum stover mulch (Figs. 2 and 3).
- When combined with MT and SRM, intercropping had no effect on soil erosion control (Fig. 3), indicating that the third component of CA, namely legume intercropping, is not always necessary; rather, the two remaining components—minimum soil disturbance and soil cover—are sufficient for controlling water erosion in the Sudan Savanna.

These findings lighten the burden of adopting CA, and thus facilitates its future promotion to the smallholder farmers in the Sudan Savanna.

(K. Ikazaki, F. Nagumo, S. Simporé [Institute of the Environment and Agricultural Research, Burkina Faso], A. Barro [Institute of the Environment and Agricultural Research, Burkina Faso])

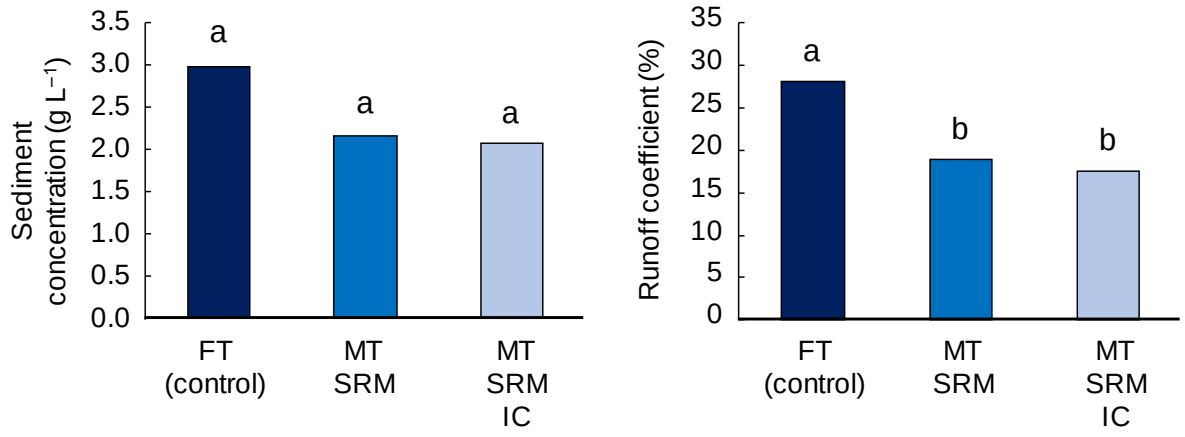

Fig. 1. Sediment concentration (left) and runoff coefficient (right) for each treatment.
FT: full tillage, MT: minimum tillage, SRM: sorghum residue mulching, IC: intercropping
Mean values with different letters are significantly different between treatments ($P < 0.05$).

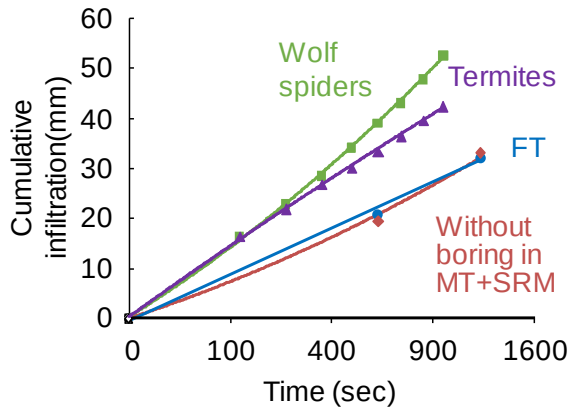

Fig. 2. Permeability of soils in full tillage plot (without animal holes) and soils with/without holes made by termites and wolf spiders in minimum tillage + sorghum residue mulching plot.

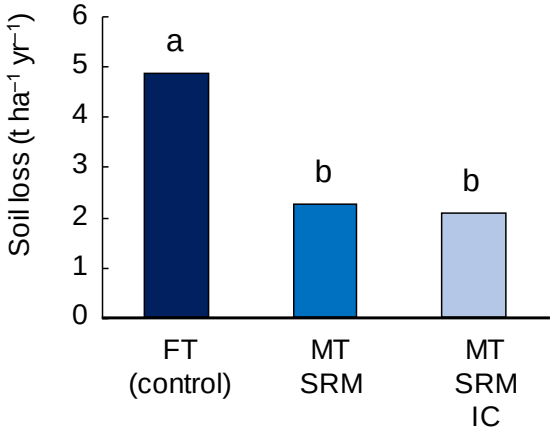

Fig. 3. Soil loss for each treatment.
Mean values with different letters are significantly different between treatments ($P < 0.05$).

Figs. 1-3 are cited from Ikazaki et al. 2018. Soil Science and Plant Nutrition, 64(2), 230-237. doi: 10.1080/00380768.2017.1422393

Non-destructive shoot biomass evaluation for field-grown staking yam (*Dioscorea rotundata* Poir)

Yam is a minor but important tuber crop grown widely in temperate to tropical regions. The total yam-cultivated area is 7.5 million hectares, with an annual harvest of 65.9 million tons of tubers. West Africa is the largest yam-cultivating area, accounting for more than 94% of the world's yam production, with *Dioscorea rotundata* being the major species used for local consumption. However, the development of varieties in this region has not benefitted from modern breeding. One reason for this slow breeding progress is the lack of phenotypic information on genetic resources due to the long growth period, low planting density, and method of reproduction (i.e., by vegetative propagation) require space, time, and effort for cultivation), thereby restricting the number of genetic resources in previous growth studies.

In this study, we developed a non-destructive method to predict shoot biomass by measuring spectral reflectance in staking yam. The normalized difference vegetation index (NDVI) was evaluated using a handheld sensor (GreenSeeker, Nikon Trimble, Tokyo, Japan) to vertically scan the plant from top to bottom along the length of the stake (Fig. 1). The scanning was carefully performed for 30 s per measurement, keeping the scan speed constant from top to bottom. To eliminate the background noise of the reflectance, a 1 m × 2 m board was placed behind the plant. A linear regression model was constructed to predict shoot biomass using NDVI as a parameter (NDVI×297.6+4.7). The observed values of shoot biomass, irrespective of the genotypes, were predicted well by the model (Fig. 2). Conversely, the model tended to underestimate the shoot biomass when the actual shoot biomass exceeded 150 g plant^{-1}; this was compensated for when the parameters of green area, calculated from plant image and plant height, were included in the model (NDVI×120.9+205.9×Green area-38.4×Plant height+40.0) (Fig. 3).

This method reduced the time, cost, effort, and field space needed for shoot biomass evaluation compared with that needed for the sampling method. The information on shoot biomass is widely available for growth analysis and for the evaluation of stress tolerance and crop models. In addition, the rapid phenotyping method fulfills the phenotypic information demands of a large number of genetic resources and cross populations. In combination with genetic tools, shoot biomass evaluation using NDVI will serve as a key method for accelerating yam breeding programs, as shown in major crops. In addition, good relationships between final tuber yield and the value of NDVI at middle growth stage were observed, indicating that this method can also be used for early prediction of tuber yield. However, the predictions were not stable among years with different meteorological conditions. Further studies are needed to clarify the relationship between tuber yield and NDVI.

(K. Iseki, R. Matsumoto [International Institute of Tropical Agriculture])

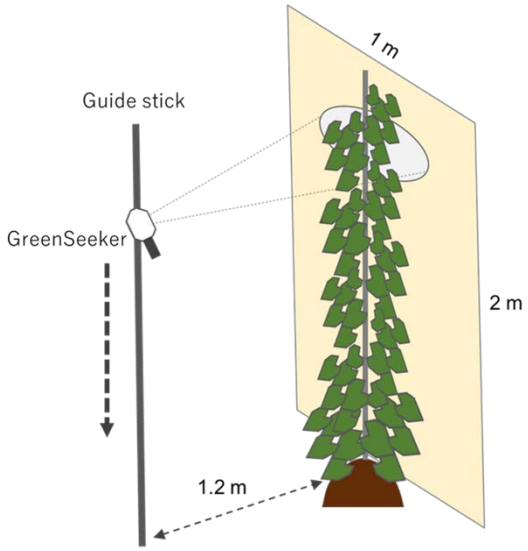

Fig. 1. NDVI measurement procedure for staking yam. The plant height was measured visually using the scale printed on the board behind the plant.

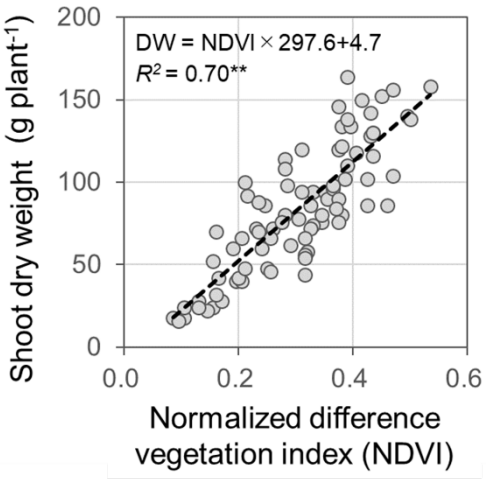

Fig. 2. Correlation between NDVI and observed shoot biomass. Model validation data of 30 yam accessions with 3 plant replications (n=90) were used. ** represents statistically significant at p = 0.01 level.

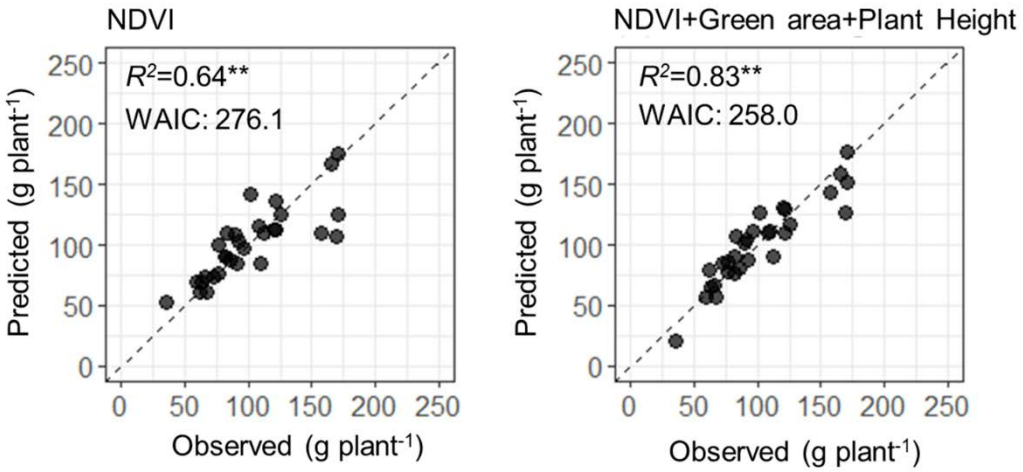

Fig. 3. Improvement of the model prediction using additional parameters of green area and plant height. Data of shoot biomass of the plants from different seed tuber size of same accession were used. Model performance was measured with the widely applicable information criterion (WAIC), where the smaller value represents better fitting. ** represents statistically significant at p = 0.01 level.

A farm management model for assisting smallholder farmers in Africa

Most farmers in Sub-Saharan Africa are smallholders. This condition threatens food security in the region as smallholders cultivate only a few hectares of farmlands and face constraints on income generation. Although there is a strong focus on new agricultural technologies and policy interventions, only a few have shed light on farm management strategies that are acceptable and feasible to smallholders for improving their diets and livelihoods. The objective of this research, therefore, is to develop a new farm management model for assisting African smallholders.

Using the linear programming approach, we constructed a farm management model that computes the optimal crop and technology choices along with the optimal scales of introducing these crops and technologies to maximize the total household income. With the necessary parameters covering farming conditions and indexes, conditions for food subsistence, and non-farm activities, the model gives a true picture of farm management optimized for African smallholders with their principal livelihood needs satisfied. These needs include 1) ensuring the area to produce enough subsistence crops for home consumption, 2) mixed cropping and intercropping as smallholders' coping strategies to production and marketing risks, and 3) ensuring non-farm income and labor distribution of farm and non-farm activities (Fig. 1). As a case study, we applied this model to smallholder farmers in the Nacala Corridor, northern Mozambique, and analyzed the optimal crop combinations in three different agroecological zones and farming scales. The results indicate that risk dispersion based on mixed cropping is effective especially in the eastern zone, which witnesses more frequent droughts and price fluctuations of agricultural products than other zones. Smallholders can also derive improved livelihoods from producing the most lucrative beans (e.g. groundnut, soybean) and tubers (e.g. sweet potato) cultivated in each zone, with the major food staples produced as well, to achieve food self-sufficiency especially among those with more than 1 ha of farmlands (Table 1). As in Figure 2, their total income could increase substantially while those with less than 1 ha have little room to increase their income because of the difficulty in meeting food self-sufficiency needs with the actual crop yields. To facilitate the model analyses, we also developed the user-friendly programs named BFMe (in English) and BFMmz (in Portuguese). Using these programs, the expected local users including agricultural extension agencies can easily implement the model to identify optimal farming plans for smallholders as well as scenarios of their technology uptake.

The model allows not only observed values but also predicted values for computation. One may use, for instance, the yields predicted using a crop model. Samples of smallholder farming in the three zones of Nacala Corridor are also available. Some may derive the optimal farming plans from using these samples for reference or change the parameters for simulation, while others may use original data collected for their own analyses.

(J. Koide, R. Yamada [Tokyo Univ of Agriculture], W. Oishi [Univ of Tsukuba], A. Nhantumbo [Agricultural Research Inst of Mozambique (IIAM)], V. Salegua [IIAM], C. Sumila [IIAM])

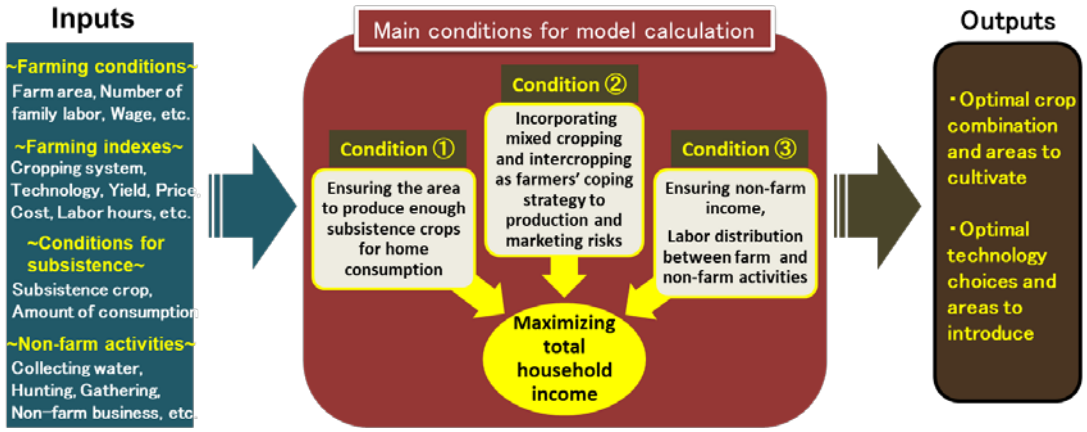

Fig. 1. A farm management model reflecting the conditions of African smallholder farming

Table 1. Optimal crop combinations in three different zones of the Nacala Corridor

		Optimal cropping area (ha)		
		I	II	III
Eastern	**Total area**	**0.68**	**1.44**	**3.05**
	Cassava+Maize+Cowpea mixed cropping	0.63	0.67	0
	Cassava+Maize+Cowpea+Peanut mixed cropping	0	0.69	2.92
	Sweet potato monocropping	0.05	0.08	0.13
Central	**Total area**	**0.67**	**1.44**	**3.6**
	Maize monocropping	0.29	0.48	0.54
	Sorghum monocropping	0.03	0.42	0.47
	Sorghum+Pigeon pea mixed cropping	0.32	0	0
	Soybean+Pigeon pea mixed cropping	0	0.54	2.59
	Rice monocropping	0.03	0.04	0.02
Western	**Total area**	**0.71**	**1.49**	**3.9**
	Maize+Common bean mixed cropping	0.65	0.85	0.95
	Sweet potato monocropping	0.06	0.64	2.95

I: Household category with less than 1 ha of farmlands. II: Household category with 1 to 2 ha of farmlands. III: Household category with more than 2 ha of farmlands. The optimal combinations consist of major crops and cropping systems identified by a field survey of 645 randomly-sampled smallholder farmers. The observed values of their farming conditions and indexes and non-farm activities are reflected into the model.

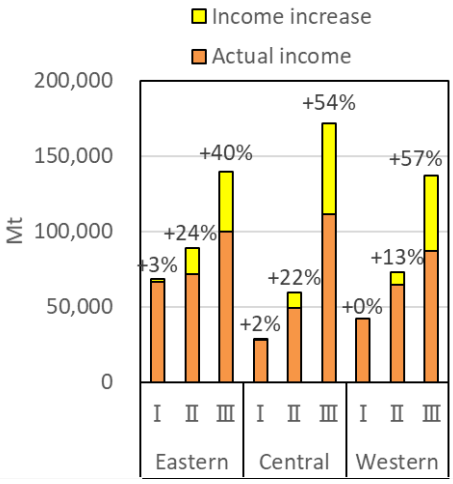

Fig. 2. Income increase by optimizing crop combinations in each zone and farming scale.

I, II, III: Same as Table 1. Mt: Metical (currency of Mozambique). Rate of income increase is indicated above the bars.

Identification of a quantitative trait locus associated with development of lateral roots in rice employing a genome-wide association study

In recent decades, lowland rice (*Oryza sativa* L.) cultivation practices have shifted away from the standard system of field puddling and transplanting towards direct seeding. Seedling vigor is an important trait for direct-seeded rice but most modern *indica* varieties were developed for transplanted rice cultivation and are therefore not expected to have good early seedling vigor. Rapid mobilization of carbon and nutrient reserves stored in the seed is an important determinant of seedling vigor; however, it needs to be supported by the rapid establishment of a root system that can supply additional nutrients and water to the seedling. In rice, nutrient and water uptake is dependent on the abundant presence of lateral roots. Our objective in this study was to map quantitative trait loci (QTL) for early lateral root development and to identify associated candidate genes.

A panel of 307 genotypes including 284 *indica* genotypes was grown in low-phosphorous nutrient solution for a 14-day period. Digital images of entire root systems were analyzed using the WinRhizo software, which provided an estimate of total root tip number present in the root system (Fig. 1A). As this figure indicates, the vast majority of root tips are tips of fine lateral roots in rice, highlighted here by yellow dots. Using genome-wide association studies (GWAS), we identified one association on chromosome 11 for root tip number (*qTIPS-11*) (Fig. 1B). The positive haplotype occurred at a low frequency (5.4%) in the panel and increased root tip number by 27.4% (Fig. 1C). The rare nature of the positive haplotype at *qTIPS-11* was confirmed in silico within the 3000 sequenced rice genomes (SNP-Seek), of which only 183 accessions, predominantly belonging to the *japonica* subspecies (71.6%), had the positive haplotype. The positive haplotype was largely absent from indica type accessions.

The putative auxin-responsive glucosyl hydrolase (*TIPS-11-9*; Os11g44950) was identified as a candidate gene (Fig. 2A) because genes responsible for cell wall hydrolysis are needed to facilitate the growth of laterals through several layers of cortical and epidermal cells during root emergence. A T-DNA knock-out mutant of *TIPS-11-9* had a 25% reduction in root tip number compared to wild-type, confirming the importance of *TIPS-11-9*. Two allelic forms of *TIPS-11-9* were detected of which the negative allele is missing the auxin response factor (ARF) (Fig. 2A). Expression of *TIPS-11-9* was induced by auxin (IAA) addition only in the positive accessions (Fig. 2B), suggesting an allele-specific response of *TIPS-11-9* to auxin. Auxin has been implicated in lateral root emergence and development, and thus *TIPS-11-9* may be involved in auxin-regulated lateral root formation or development, or both.

Marker-assisted introgression of *qTIPS-11* into modern *indica* varieties will aid in the generation of varieties adapted to direct seeding and to nutrient-limited environments. Clarification of the functions of *qTIPS-11* throughout the life cycle of rice will be required.

(M. Wissuwa, F. Wang, T. Ishizaki, J.P. Tanaka, T. Kretzschmar [International Rice Research Institute])

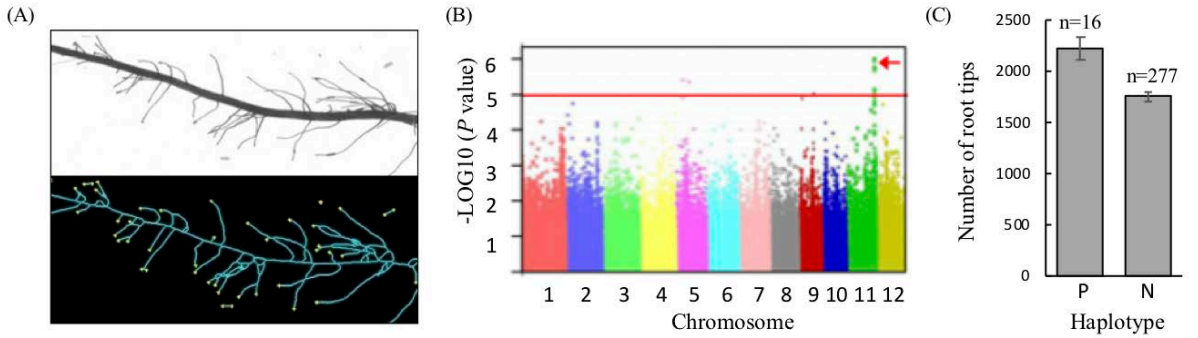

Fig. 1. Detection of a QTL related to lateral root development through GWAS.
(A) Example of digital image analysis of a root segment with scanned image (top) and processed image with root tips indicated by yellow dots (bottom). (B) Manhattan plot indicating significant association between SNP markers on all 12 chromosomes of rice and root tip number. The vertical axis indicates the strength of this association with a threshold set at P = 1.0E-05. (C) Difference between positive (P) and negative (N) haplotypes at *qTIPS-11* on root tip number.

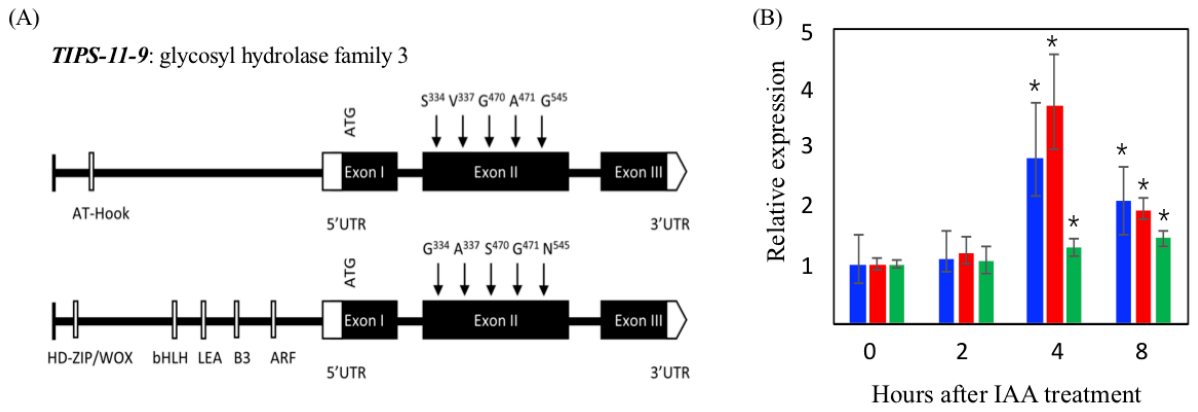

Fig. 2. Characterization of candidate gene *TIPS-11-9* for lateral root development at *qTIPS-11*.
(A) Allelic differences for *TIPS-11-9* with negative allele (top) and positive allele (bottom). The positive allele contains an auxin response factor (ARF). (B) Expression of *TIPS-11-9* in roots of *qTIPS-11* positive accessions Milyang 30 (blue) and Kitaake (red), relative to expression in the negative accession Cauvery (green) in response to auxin (IAA) addition to the rooting medium. Gene expression is shown relative to expression in Cauvery at 0 hours.

Development of wild soybean chromosome segment substitution lines for genetic studies of important traits

Wild soybean (*Glycine soja* Sieb. & Zucc.) is believed to be the progenitor of cultivated soybean (*G. max* (L.) Merr.). It has been revealed that wild soybean has higher genetic diversity than cultivated soybean, presenting a potential genetic resource pool for improvement of the latter. However, the inheritance mode of many important agronomic traits, such as seed quality, grain yield, and tolerance to environmental stresses, is extremely complex, and their performances are greatly affected by the genetic background and growth environment, making it difficult to identify the useful genes possessed by wild soybean. In this study, we created wild soybean chromosome segment substitution lines (CSSLs), in which the cultivated soybean chromosomes were replaced by only one or a few small chromosome segments of wild soybean, and thus these lines have similar genetic background but differ only in the small wild soybean chromosome region(s). We employed the CSSLs for genetic analysis of some important agronomic traits in soybean and demonstrated that the CSSLs might accelerate the identification of useful genes in wild soybean.

A total of 120 BC_3F_5 CSSLs were developed from a cross between the cultivated soybean variety 'Jackson' and the wild soybean accession 'JWS156-1.' These lines were created by backcrossing of {[(('Jackson' × 'JWS156-1') × 'Jackson') × 'Jackson'] × 'Jackson'} and five successive generations of self-pollination without any selection. A total of 235 SSR soybean markers from all 20 chromosomes were used for genotyping the 120 CSSLs. The proportion of the recurrent parent 'Jackson' alleles in each CSSL ranged from 80.3% to 99.2% with an average of 92.9 ± 4.0%, which corresponded to the expected value, 93.8% (Fig. 1).

To identify the quantitative trait locus (QTL) of seed weight, which is one of the most important traits that control soybean yield, the 120 CSSLs were cultivated in field conditions over three years and the seed weight trait was measured for each CSSL. QTL analysis detected nine QTLs (*qSW8.1*, *qSW9.1*, *qSW12.1*, *qSW13.1*, *qSW14.1*, *qSW16.1*, *qSW17.1*, *qSW17.2*, and *qSW20.1*) on eight chromosomes. Of these, *qSW12.1* was detected over the three successive years on a region of 1,348 kb in chromosome 12 as a novel, stable, and major seed weight QTL (Fig. 2).

In order to identify new flowering time QTLs, we evaluated the 120 CSSLs over two years under field conditions. Four QTLs (*qFT07.1*, *qFT12.1*, *qFT12.2*, and *qFT19.1*) were detected on three chromosomes. Of these, *qFT12.1* showed the highest effect, accounting for 36.37–38.27% of the total phenotypic variation over two years. *qFT12.1* may be a new flowering time gene locus in soybean (Fig. 3).

In our study, a BC_3F_5 CSSL population has been developed. Since some CSSLs still has wild soybean segments or heterozygous regions other than the target wild soybean substitution segment, further backcrossing and DNA marker selection are needed for eliminating such redundant wild segments in the CSSLs. Nevertheless, the developed CSSL population has potential for mining useful genes in wild soybean.

(D. Xu, Y. Fujita, D. Liu)

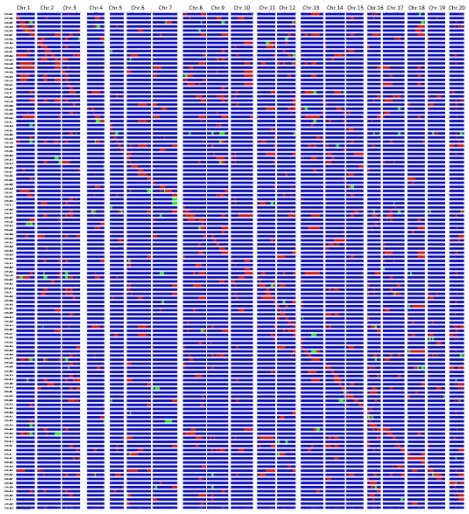

Fig. 1. Graphical genotypes of the wild soybean 'JWS156-1' chromosome segment substitution lines (CSSLs) in the cultivated soybean variety 'Jackson' background. Red: 'JWS156-1' homozygous, blue: 'Jackson' homozygous, green: heterozygous. This figure is modified from Liu D et al. (2018a) (Copyright: Japanese Society of Breeding).

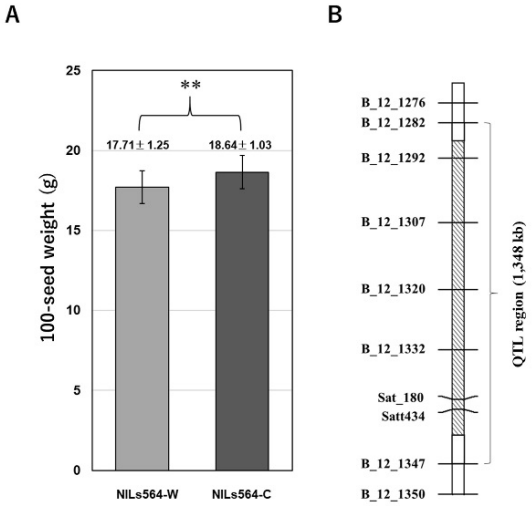

Fig. 2. Seed weight QTL *qSW12.1* detected in the wild soybean CSSLs population.

(A) The allele effect of *qSW12.1* in near-isogenic lines NILs564-C ('Jackson' genotype) and NILs564-W ('JWS156-1' genotype). Data are shown as means ± SD (standard deviation). **: $P < 0.01$. (B) *qSW12.1* was delimited in a 1,348-kb interval on chromosome 12. This figure is modified from Liu D et al. (2018a) (Copyright: Japanese Society of Breeding).

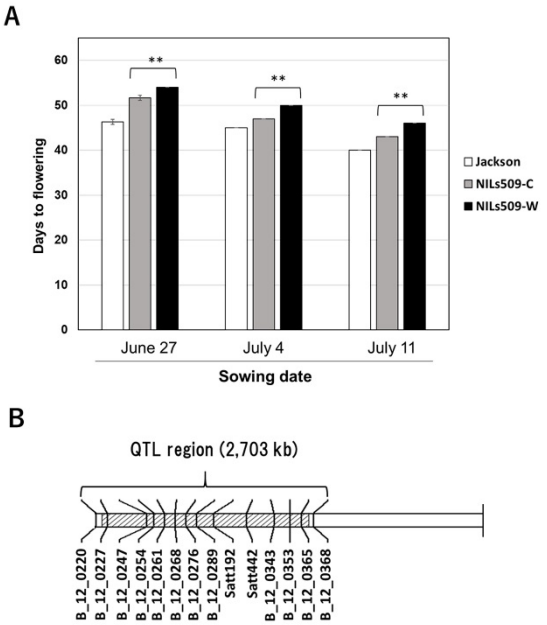

Fig. 3. Flowering time QTL *qFT12.1* detected in the wild soybean CSSL population

(A) Allelic effects of *qFT12.1* in near-isogenic lines (NILs) sown in the field on different dates in 2017. NILs509-C: 'Jackson' genotype, NILs509-W: 'JWS156-1' genotype. Data are shown as means ± SD (standard deviation). **: $P < 0.01$. (B) *qFT12.1* was delimited in a 2,703-kb interval on chromosome 12. This figure is modified from Liu D et al. (2018b) (Copyright: Springer Science + Business Media B.V.).

Accelerating soybean breeding in a CO_2-supplemented growth chamber

Soybean (*Glycine max* L. Merr.) originated in East Asia, including Japan, and is the most important dicot crop worldwide. Soybean is increasingly used as a model legume due to the availability of genomic resources in this species, and the decreasing cost of sequencing has further encouraged plant researchers to shift their focus from model plants to soybean. Nonetheless, the long generation times of this crop pose a major obstacle to soybean research and breeding. Recently, Watson et al. (2018, *Nature Plants*) reported a speed breeding method for reducing the generation times of long-day crops such as wheat and barley using a prolonged photoperiod; however, no useful methods for speed breeding short-day soybean plants have currently been published.

Here, we demonstrate a method for accelerating soybean breeding in the compact growth chambers (internal volumes of approximately 0.4 m^3) with fluorescent lamps (220 µmol m^{-2} s^{-1} at the canopy level) commonly used for laboratory research, which facilitate soybean breeding and research projects. We utilized the 14-h light (30°C)/10-h dark (25°C) cycle, which reduced flowering time, and the immature seeds to reduce reproductive phase. Additionally, supplementation of carbon dioxide (CO_2) over 400 ppm promoted soybean growth, yield, and number of healthy flowers, and thus our method also facilitates the highly efficient and controlled crossing of soybean plants. Using this approach, the generation time of the best-characterized elite Japanese soybean cultivar, Enrei, was shortened to just 70 days, thereby allowing up to 5 generations per year with efficient crossing instead of the 1–2 generations currently possible in the field and/or greenhouse.

Thus, CO_2 supplementation and appropriate light and temperature conditions combined with immature seeds enable the acceleration of soybean breeding in the compact growth chambers. Given that each soybean cultivar can be cultivated only in limited latitudes, the photoperiod conditions among the parameters in our method needs to be adapted for each cultivar. Alongside other protocols for speed breeding and effective phenotyping, the parameters used in our method could be optimized for a variety of species, cultivars, accessions, and experimental designs to facilitate cutting-edge breeding in a wide range of crops.

(Y. Nagatoshi, Y. Fujita)

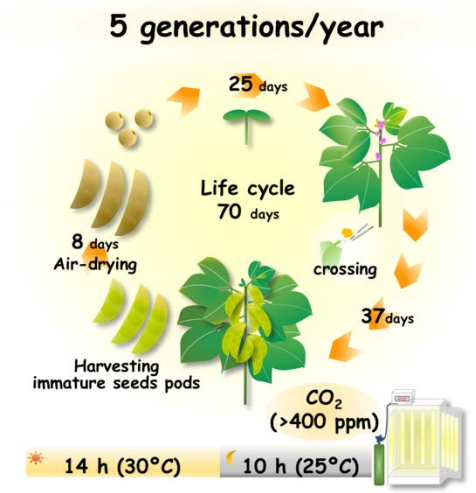

Fig 1. Schematic representation of our method for accelerating breeding in soybean (cv. Enrei) in a growth chamber supplemented with CO_2.

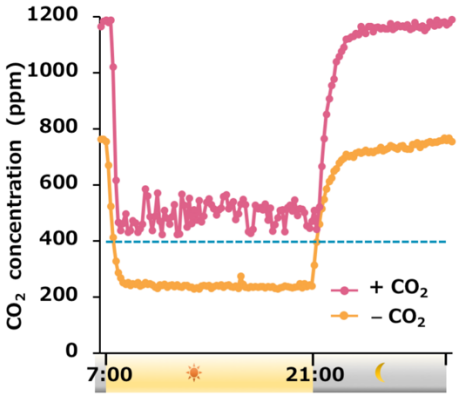

Fig 2. The internal CO_2 concentrations within growth chambers containing soybean plants are decreased during light periods.

The data were collected every 10 minutes over a single day, 25 days after flower initiation in the soybean plants.

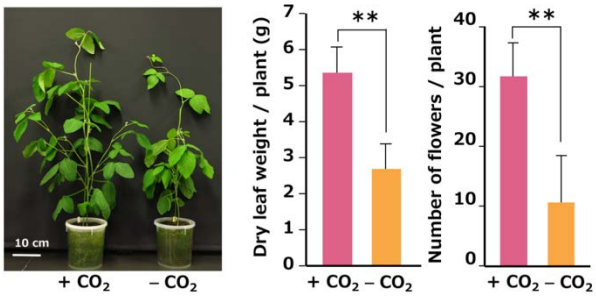

Fig 3. CO_2 supplementation enhances soybean growth and flower number in growth chambers.

Images show 31-day-old soybean plants.

The graphs show the dry leaf weight per plant at 31 days after sowing, and the number of healthy flowers produced during the first 5 days of flowering in growth chambers. (n = 4, Bar = SD. $^{**}p < 0.01$).

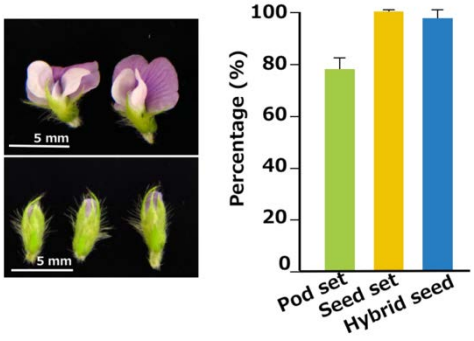

Fig 4. The soybean flowers grown in the CO_2-supplemented growth chamber are useful for effective crossing.

Images show flowers (upper) and flower buds (lower) of soybean plants grown in the CO_2-supplemented growth chamber. The graph shows the crossing efficiencies in soybean plants grown in CO_2-supplemented growth chambers. (n = 36, Bar = SD.)

Development of intergeneric F_1 hybrids between sugarcane and *Erianthus arundinaceus* as a new sugarcane breeding material

Sugarcane (*Saccharum* spp. hybrid) is an important crop for food and energy production, and further improvement of its productivity will contribute to promoting food sustainability and energy security around the world. However, its narrow genetic base has hindered the improvement of its productivity through breeding. For further improvement of sugarcane, broadening its genetic base by the introduction of new genetic resources is essential. *Erianthus arundinaceus*, a close relative, shows considerable potential as breeding material for sugarcane improvement owing to its high biomass productivity and exceptional adaptability to biotic and abiotic stresses. The aim of this study was to develop intergeneric F_1 hybrids between sugarcane and *E. arundinaceus*, and to evaluate their cytogenetic and agronomic characteristics for their effective utilization in sugarcane breeding.

From crosses between Japanese sugarcane variety NiF8 (2n = 110, female) and *E. arundinaceus* (2n = 60, male), we identified 39 hybrids by amplification of 5S rDNA markers and 2 hybrids by morphological characteristics (Fig. 1). The number of *Erianthus* chromosomes in the hybrids varied from 18 to 29, even though “n + n” parental chromosome transmission occurred (Fig. 2). Some hybrids showed intra-clonal variation in *Erianthus* chromosome number between vegetatively propagated clones, and some hybrids could not be identified by 5S rDNA markers owing to the elimination of the *Erianthus* chromosomes with the 5S rDNA loci (Fig. 2). The number of *Erianthus* chromosomes in the intergeneric hybrids was strongly correlated with their DNA content, suggesting the possibility of estimating the number of *Erianthus* chromosomes in the hybrids from their DNA content (Fig. 3). Many hybrids showed “hybrid weakness” in yield-related characteristics, and their sucrose and fiber contents were comparable with the mid-parent values (Table 1). The number of *Erianthus* chromosomes in the hybrids was significantly positively correlated with some yield-related characteristics but not quality-related characteristics (Table 1). These hybrids showed high genetic coefficient of variance in agronomic characteristics, so the selection and utilization of hybrids with higher yields or higher sugar contents is possible (Table 1, Fig. 1).

The intergeneric F_1 hybrids developed in this study provide new materials for broadening the genetic base of sugarcane. The detailed information on their cytogenetic and agronomic characteristics will contribute to effective utilization of *Erianthus* in sugarcane breeding.

(Y. Terajima, H. Takagi, P. Babil [Tokyo University of Agriculture], N. Ohmido [Kobe University], M. Ebina [National Agriculture and Food Research Organization], S. Irei [Okinawa Prefectural Agricultural Research Center], H. Hayashi [University of Tsukuba])

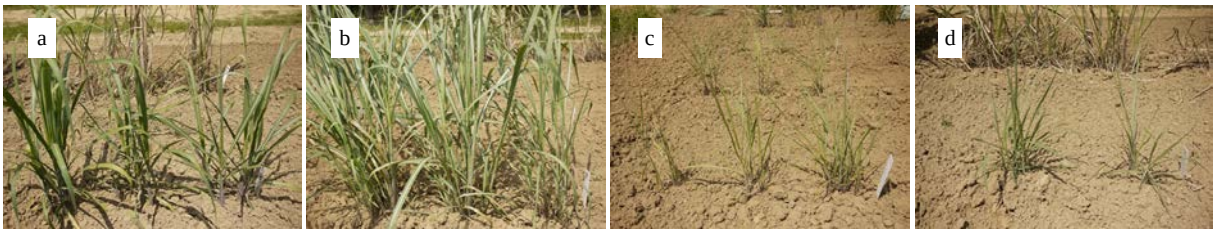

Fig. 1. Growth of intergeneric hybrids between sugarcane and *E. arundinaceus*

a: NiF8 (*Saccharum* spp. hybrid, female parent), b: J08-12 (intergeneric hybrid with no hybrid weakness), c: J11-14 (intergeneric hybrid with hybrid weakness), d: J09-2 (intergeneric hybrid selected by morphological characteristics). These pictures were taken on 8 May 2013 in the ratooning field at JIRCAS-TARF.

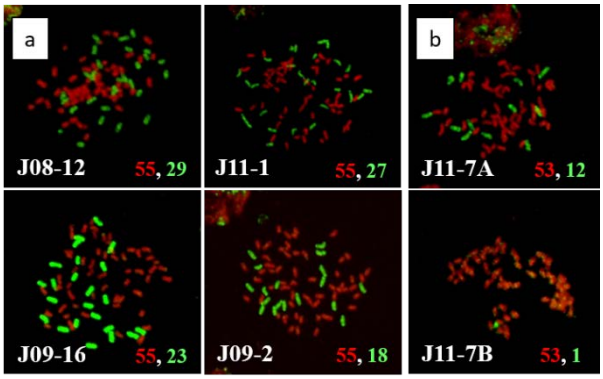

Fig. 2. GISH analysis of intergeneric hybrids

a: Variation of chromosome composition among hybrids. b: Variation of *Erianthus* chromosome number in vegetatively propagated clones of J11-7. J08-12, J11-1, J09-16 and J11-7 were screened by 5S rDNA but J09-2 was identified by morphological characteristics. Numbers in the bottom right corner indicate *Saccharum* (red) and *Erianthus* (green) chromosome number.

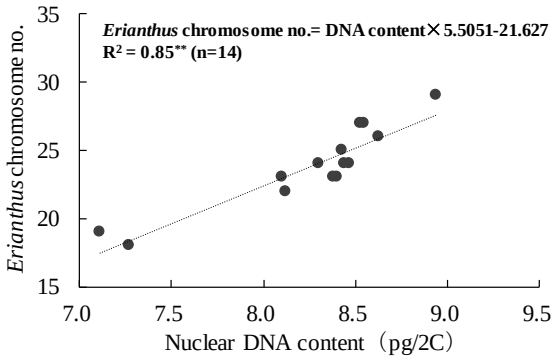

Fig. 3. Correlation between the nuclear DNA content and *Erianthus* chromosome number in intergeneric hybrids

The data of 14 intergeneric hybrids with no intra-clonal variation in 5S rDNA sites were used.

Table 1. Agronomic characteristics of intergeneric hybrids (New planting)

Characteristic	NiF8 Sugarcane (Female)	JW4 *Erianthus* (Male)	Intergeneric hybrids Average (n=32)	Min. (n=32)	Max. (n=32)	CV_g (n=23)[1)]	Correlation with *Erianthus* chromosome no. (n=14)[2)]
Dry matter yield (g/stool)	1621.9	1419.3	591.0	40.3	1713.2	68.6	0.773*
Number of stalks (no./stool)	6.4	43.4	10.8	1.0	22.1	40.2	0.336
Stalk length (cm)	119.5	64.8	67.6	15.0	125.8	39.5	0.457
Stalk diameter (mm)	21.8	10.7	12.1	5.9	16.6	17.4	0.697*
Sucrose content (%)	17.8	3.1	8.5	2.3	18.0	20.4	0.418
Fiber content (%)	10.2	23.4	16.7	8.0	22.4	15.1	-0.409

The evaluation of agronomic characteristics was conducted at JIRCAS-TARF. The seedlings of 32 intergeneric hybrids were transplanted in the experimental field on 22 May 2012 and harvested between the 18 and 22 February 2013. Five stools per plot (2.8 m^2) with three replicates placed according to a randomized block design were prepared for 23 intergeneric hybrids and the parental varieties. Six hybrids were replicated twice and three others only once due to difficulties with multiplication. 1): Analysis of the genetic coefficient of variance (CVg) were performed using data for the 23 hybrids for which three replicates were available. 2): The data of 14 intergeneric hybrids with no intra-clonal variation in 5S rDNA sites were used. *Significance at a 5% level.

Spatiotemporal distribution patterns of the desert locust in Africa

The desert locust, *Schistocerca gregaria*, is one of the most destructive pests in the world. Sometimes, desert locust populations grow explosively, forming swarms and causing locust plagues. A plague can affect up to 20% of the earth's surface across Africa, the Middle East, and Southwest Asia. Desert locusts can potentially damage the livelihoods of a tenth of the world's population. The preventive approach involves monitoring and spraying of locust breeding areas. However, this is difficult in practice as many of the principal breeding zones are in remote areas and difficult to reach. Despite these constraints, we will keep studying the locust and aim for efficient and sustainable control measures with due consideration to environmental well-being. We have learned, for example, that gregarious locusts can form a dense group at certain sites within a day. If we can understand these spatiotemporal aggregation patterns, we can control locusts efficiently using only small amounts of pesticides. To obtain these ecological data, we have conducted field surveys in Mauritania in collaboration with the Mauritanian National Anti-Locust Center.

In the field, actively marching migratory bands of gregarious nymphs passed some plants before finally roosting and aggregating on patchily distributed trees around dusk (Fig. 1). Migratory bands formed the largest group on the largest tree within the local plant community (Fig. 2). They apparently chose the largest plants. Adults similarly roosted on large trees or medium-sized bushes (Fig. 3). Flight escape was the preferred defense when temperatures were above the minimum threshold for locust flight (22 °C). At low temperatures, defense response to predator threat varied with plant size and locust height off the ground: locusts in low bushes dropped to the center of the bush and hid, whereas those above 2 m in trees remained stationary. These alternative defense behaviors appear to be adaptive under the different environmental conditions. Flight escape is extremely effective but cannot be performed under 22 °C. Hence, alternative defenses (dropping or remaining stationary) are necessary. These defenses are effective at low temperatures because dynamic locomotion is not required.

Our results suggest that desert locusts integrate information about microhabitat, temperature, and threat characteristics to adaptively adjust defense tactics. Control operation and monitoring should consider these ecological characteristics especially because this plant-size-dependent roosting site choice during the night may contribute to the development of artificial trapping systems for locusts and a shift to a new environment-friendly, night control approach.

(K. Maeno, S. Ould Mohamed [The Mauritanian National Anti-Locust Centre])

Fig. 1. Night-roosting site choice by gregarious nymphs of *Schistocerca gregaria.*
Arrow indicates the largest tree roosted on by the largest locust group.

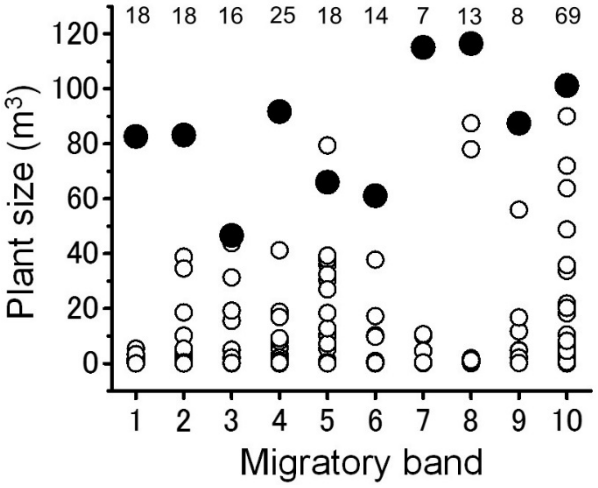

Fig. 2. Plant-size distribution at each site where 10 migratory bands of *Schistocerca gregaria* roosted.
Closed circles indicate the plants roosted on by the largest locust group (the center) and open circles indicate other individual plants in the local site (within 20 m from the center). The largest aggregation formed on the largest tree within the plant community in nine of the ten bands. Figures at the top indicate the numbers of plants examined.

Fig. 3. Adult locusts roosting on the branches of a large tree during the night.

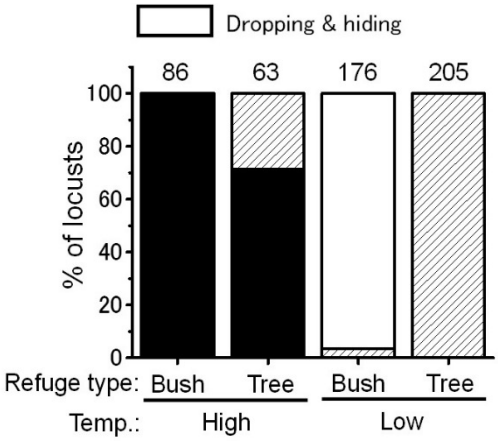

Fig. 4. Defensive responses exhibited by adults including flying, stationary, and dropping and hiding by using plants as a refuge.
Adults perched on small bushes (< 1.5 m height) or large trees (> 2 m height) in the morning (07:30–08:30) when the ambient temperature was either higher or lower than their critical body temperature for flight (22 °C). Figures at the top indicate sample sizes.

Estimation of rice grain yield by canopy hyperspectral sensing of paddy fields at the booting stage

Remote sensing is a promising tool for assessing growth status and predicting rice yield. Recent advances in unmanned aerial vehicles (UAVs) and sensor technologies have enabled farmers to frequently observe the paddy fields at low-altitudes. However, the optimal timing of UAV observations and the suitable sensor specifications for yield prediction are not clearly understood. Therefore, with the aim of improving UAV utilization for the future, field hyperspectral (HS) measurement at canopy scale was performed in a paddy field, and the optimum growth stage and spectral waveband for yield prediction were clarified.

The experimental results are summarized as follows:

- Canopy hyperspectral measurements were conducted at different growth stages (Fig. 1, T1: Panicle initiation, T2: Booting stage, and T3: Milk stage) in an experimental paddy field where six Lao rice cultivars were tested with three replicates at the Rice Research Center (RRC) of the National Agriculture and Forestry Research Institute (NAFRI), Laos. Partial least squares (PLS) regression analyses that were not affected by the collinearity of HS data (400–930 nm, 531 bands) were performed to predict grain yield of rice. The predictive accuracies at three different growth stages were compared.
- Among the three growth stages, the highest values for predictive accuracy (R^2 = 0.843) and reproducibility of the model (RPD > 2.43) were obtained at the booting stage (Fig. 2).
- Although the predictive accuracy and reproducibility values were low (R^2 = 0.479, RPD = 1.316), the grain yield was predicted in the panicle initiation stage (Fig. 2).
- Grain yield might be difficult to predict after the milk stage when the rice plant's leaf color turns yellow (Fig. 2).
- Based on the selected wavebands in the PLS model at booting stage when the growth reaches its peak, the red-edge (700–760 nm) and near-infrared (810–820 nm) wavelength regions were selected as important wavebands for yield prediction (Fig. 3). These wavelengths are previously known to be closely related to plant aboveground biomass and nitrogen content, and they can be used to estimate the nutritional status of rice.

These results indicated that grain yield of rice could be predicted with practical accuracy by field HS measurement at the booting stage. Such timely and accurate rice yield assessments approximately one month prior to harvest will enable staffs at the regional agriculture and forestry offices and parties concerned with the rice market to quantify rice production, supply and market prices. Moreover, by installing a camera capable of measuring the red-edge and near-infrared wavelengths on UAVs, it may be possible to forecast yield over a wide area. It should be noted, however, that further analysis is required to verify whether similar results can be obtained for cultivars in other areas, especially those with large differences in traits (e.g. plant height)

(K. Kawamura, H. Ikeura, S. Phongchanmaixay [NAFRI, Laos])

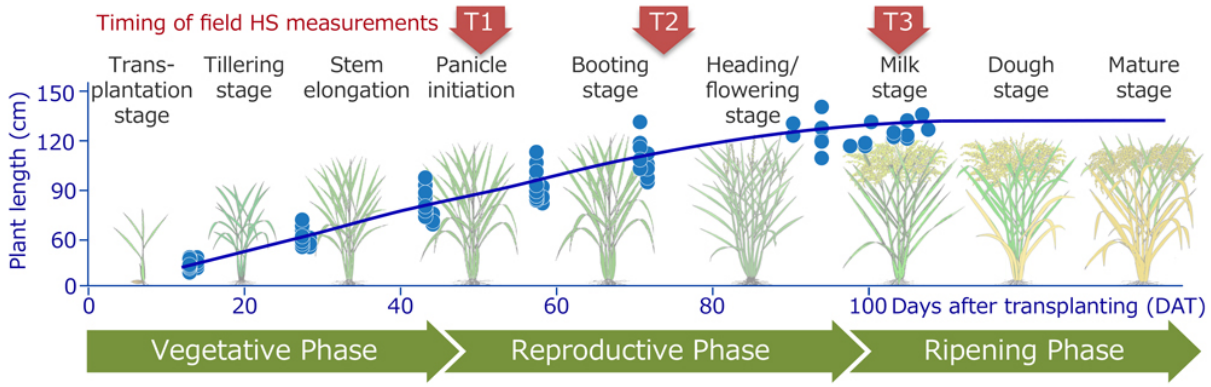

Fig. 1. Plant height and the timing of field HS measurements at different growth stages in a paddy field.

Source of rice plant image data: http://www.knowledgebank.irri.org/decision-tools/growth-stages-and-important-management-factors

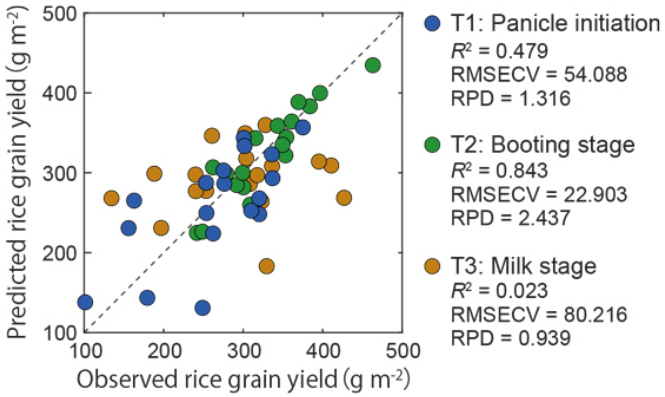

Fig. 2. Observed and predicted values of rice grain yield using PLS regression for datasets T1, T2, and T3 (n = 18).

RMSECV: Root mean squared errors of cross-validation using leave-one-out method.

RPD: Residual predictive deviation. The criteria for determination are (1) RPD < 1.15: unpredictable, (2) 1.16–1.40: weakly correlated, (3) 1.71–2.42: capable of screening, and (5) >2.43: possible to estimate with practical accuracy.

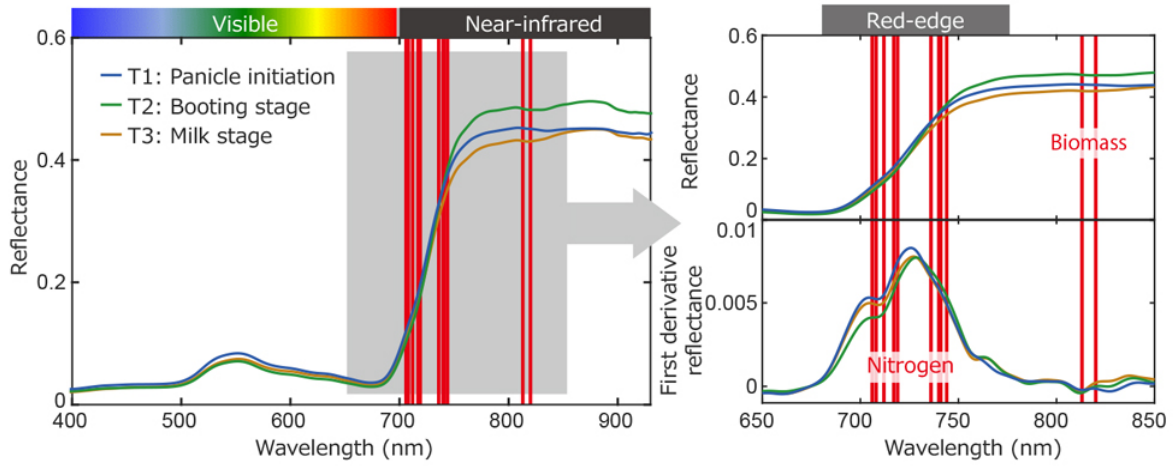

Fig. 3. Canopy reflectance and selected wavebands (red bars) in the ISE-PLS model for booting stage (T2).

Herbivorax saccincola A7, a novel alkaliphilic and thermophilic anaerobe, effectively degrades xylan-rich lignocellulosic biomass

Highly efficient degradation of lignocellulosic materials (which contain a mixture of cellulose, hemicellulose, and lignin) by biological saccharification is required for developing a cost-effective method of producing fuel and chemicals from biomass. The known thermophilic anaerobes *Clostridium thermocellum* and *C. clariflavum* can degrade and assimilate cellulose. However, these species cannot utilize xylan, which is the main component of hemicellulose contained in lignocellulosic biomass. The amount of cellulose and hemicellulose in lignocellulosic biomass is similar, hence we explored and isolated a novel thermophilic anaerobe for its ability to degrade and assimilate both cellulose and xylan from a cellulose-degrading bacterial community inhabiting bovine manure compost in Ishigaki Island, Japan (Fig. 1A).

This strain was identified as *Herbivorax saccincola* A7 (hereinafter referred to as A7) based on 16S rRNA gene sequence similarity. A7 is closely related to the cellulose-degrading bacteria of *C. thermocellum* and *C. clariflavum* in the family *Ruminococcaceae* (Fig. 1B). The optimal growth pH of A7 was alkaline pH 9.0, but *C. thermocellum*'s and *C. clariflavum*'s are at around neutral pH (Table 1). The genome size of A7 was 3.76 Mb with a G + C content of 34.9%. The genome contained 3346 protein-coding regions, nine rRNA genes, and 54 tRNA genes from a total of 3642 genes (Table 1). The 38 genes encoding glycosyl hydrolase were contained in the A7 genome. The ratio of xylanase to all glycosyl hydrolase was higher in A7 than in *C. thermocellum* and *C. clariflavum* (Table 1). In addition, A7 has genes that encode related protein to the metabolic pathway of xylose and xylooligosaccharide and for their uptake; *C. thermocellum* and *C. clariflavum*, on the other hand, do not possess these genes (Fig. 2). The metabolic pathway and transporters of xylose and xylooligosaccharide would enable A7 to assimilate xylan.

A7 can degrade lignocellulose biomass at alkaline and high temperature conditions, lowering the risk of bacterial contamination. In addition, the alkaliphilic microbe A7 can tolerate pH decrease with organic acid production by fermentation, sustaining the degradation activity longer than neutrophilic cellulose-degrading bacteria. As mentioned earlier, A7 can also assimilate xylan, thus this strain has great potential to effectively degrade xylan-rich lignocellulosic biomass such as empty fruit bunch, oil palm trunk, and corn stover (Patent application number PCT/JP2017/021784). A7 can be obtained from the Leibniz Institute DSMZ - German Collection of Microorganisms and Cell Cultures (Deutsche Sammlung von Mikroorganismen und Zellkulturen GmbH) and the Japan Collection of Microorganisms (JCM), RIKEN BioResource Center (RIKEN BRC).

(S. Aikawa, A. Kosugi)

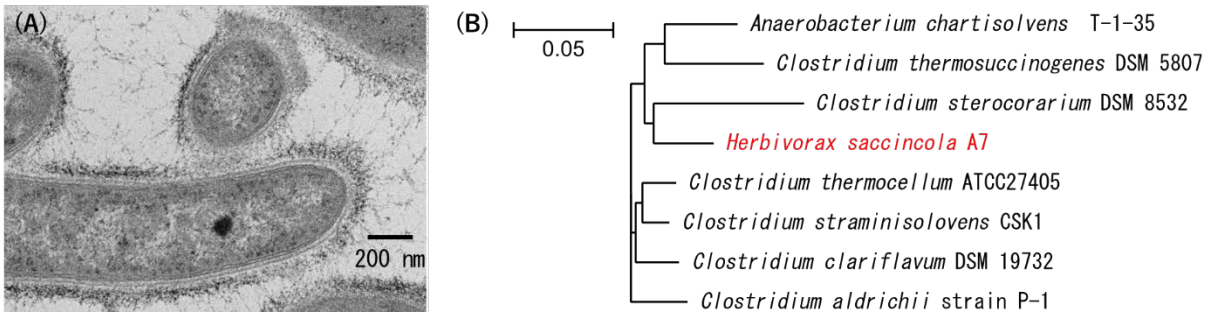

Fig. 1. Electron micrograph (A) and phylogenetic tree (B) of *H. saccincola* A7.

Black-colored bar in photograph is 200 nm long.

Black-colored bar at the upper left of phylogenetic tree shows the ration of different base sequence (0.05).

Table 1. Physiological properties and comparative genome analysis of *H. saccincola* A7 with related species

Characteristic	*H. saccincola* A7	*C. clariflavum* DSM 19732	*C. thermocellum* ATCC27405
Optimal growth pH	9	7.5	7
Xylan assimilation	Yes	No	No
Genome size［Mb］	3.76	4.9	3.84
Total number of genes[*1]	3,346	3,906	3,204
Total number of glycolytic enzymes[*2]	38	47	42
Number of xylanases	8 (21%)[*3]	6 (12%)[*3]	1 (2%)[*3]

[*1] Total number of protein coding genes

[*2] Total number of glycosyl hydrolases containing cellulase, xylanase, and other activities

[*3] Percentages in parentheses show the ratio of xylanase to total glycosyl hydrolases.

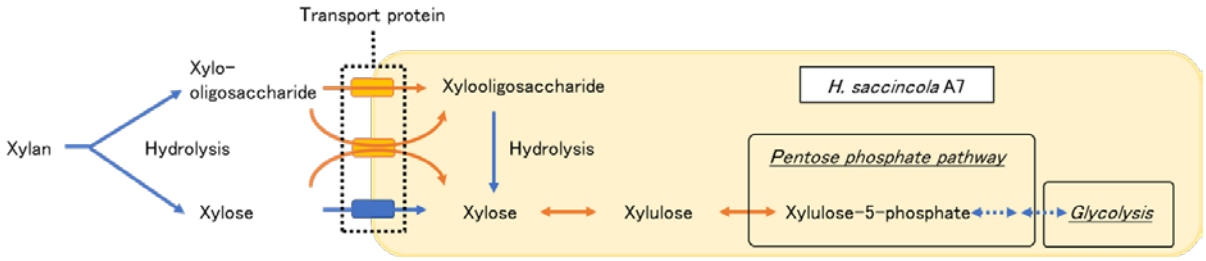

Fig. 2. Metabolic pathway of xylose and xylooligosaccharides in *H. saccincola* A7.

Orange-colored pathways are specific genes in A7 and blue-colored pathways are possessed in common among related species.

Climbing perch aquaculture is realizable in rice paddies under non-feeding conditions by rearing at low stocking densities

In Laos, national food demand has been increasing due to population growth, and animal protein deficiency among residents of mountainous rural areas is an important national concern. To improve this situation, fish aquaculture has been promoted but current major targets for aquaculture, e.g., the Nile tilapia and carps, are introduced species and further development of their aquaculture may cause great risks to biodiversity conservation in the area. In addition, the residents in such rural areas are economically deprived and cannot afford to build specific aquaculture infrastructures, e.g., culture cages and ponds. Therefore, we examined the feasibility of fish culture in a rice paddy (rice-fish culture) using a Laotian indigenous fish, the climbing perch (*Anabas testudineus*, Fig. 1), without investing in specific infrastructures, and we analyzed/evaluated several factors relevant to fish productivity in a rice-fish culture system.

Through four experimental culture trials in Nameuang and Napoh villages during 2013-2016, feeding condition (feeding or non-feeding), stocking density of fingerlings (fish/m^2), stocking period (days) and fish size at stocking (g/fish) were analyzed as potential contributory factors to the BGI (biomass gain index = total weight of fish at stocking / total weight of fish at harvest). We conducted linear regression analyses using all the combinations of the above four parameters. Feeding condition (F), stocking density (SD), and stocking period (SP) were eventually selected as contributory factors, while fish size at stocking (BW) was excluded (Fig. 2). Thereafter, we evaluated the contributory effects of each parameter by the regression coefficients of the model as $BGI = -27.9 \cdot SD - 0.53 \cdot SP + 6.07 \cdot F + 108.9$ ($R^2 = 0.96$) and found that stocking density was the most important contributory factor and that high BGI can be expected if reared at a low stocking density even under non-feeding condition (Fig. 3). Feeding condition was revealed to be a secondary contributory factor, with better BGI expectable under feeding condition than non-feeding condition. Stocking period's contribution to the BGI, on the other hand, was limited compared to the above two factors (Fig. 3). Based on the above analyses, high BGI (BGI ca. 40, or 40kg expectable harvest weight over 1kg fingerling weight at stocking) is the realizable fish productivity under feeding condition for the rice-fish (climbing perch) culture system, even as acceptable BGI (BGI ca. 20) is still expectable even under non-feeding condition if reared at a low stocking density (< 1 fish/m^2) (Fig. 4).

Assuming that rice-fish culture can be extended across the country, we have estimated ca. 84,000 ha of full-time ponded rice paddies that may be utilized to produce ca. 21,000~42,000t of fish by rice-fish culture. However, the infrastructures and the number of technical staffs for aquacultural fingerling production are largely insufficient, and obtaining the required quantity/supply of fingerlings is currently not possible in Laos. Prompt enhancements are thus necessary to overcome these constraints.

(S. Morioka, K. Kawamura, B. Vongvichith [Living Aquatic Resources Research Center])

Fig. 1. Rice paddy for fish culture (top) and the harvested climbing perch (bottom)

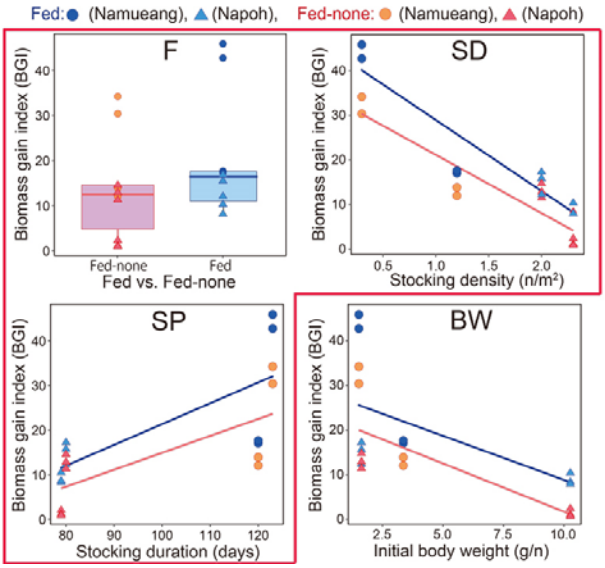

Fig. 2. Potential factors relevant to fish productivity (BGI) in a rice paddy.
[F: feeding or non-feeding, SD: stocking density of fingerlings, SP: stocking period, BW: weight of fingerling at stocking. F, SD & SP were selected as influential parameters by linear regression analyses, while BW was not selected]

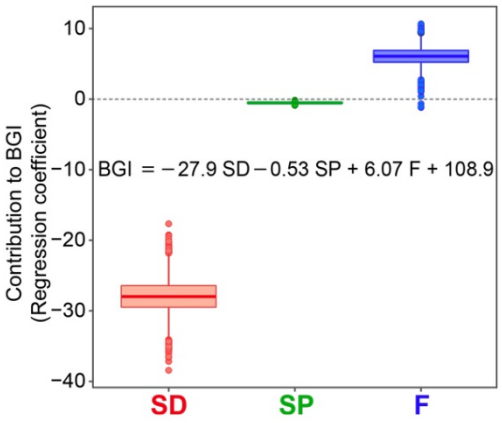

Fig. 3. Evaluation of the contribution of selected parameters [stocking density (SD), stocking period (SP), and feeding condition (F)] to fish productivity (BGI)

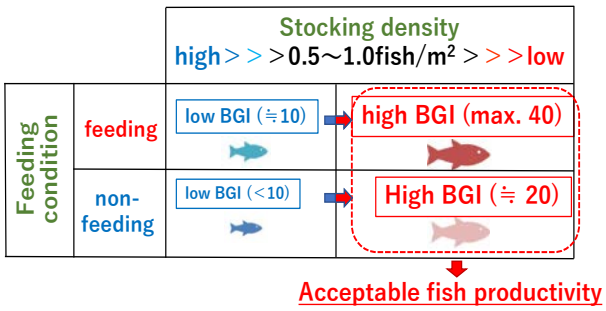

Fig. 4. Schematic image of the effects of stocking density and feeding condition as contributory factors to fish productivity (BGI)

Increasing rainy season lowland rice and dry season crop yields in the semi-mountainous villages of Laos using stored water intended for aquaculture

Agricultural fields in the semi-mountainous villages of Laos depend heavily on rainwater. Past water shortages had delayed transplanting of rainy season lowland rice in the lower parts of the fields (Fig. 1), leading to low yields (www.jircas.go.jp/ja/publication/research_highlights/2015). Moreover, crop cultivation in the dry season has not been conducted due to little precipitation. To complete earlier transplanting and conduct dry season cropping, it is necessary to introduce preparatory irrigation in early rainy season (PIR), and supplemental irrigation in the dry season (SID). Six reservoirs were constructed for aquaculture at N Village in the northwestern part of Vientiane Province, with 8,600 m^3 of stored water left unused due to structural issues with the reservoir outlet (Fig. 2). This study aims to formulate a water management plan that includes the introduction of PIR and SID through usage of stored water. It also shows the potential irrigation areas for PIR and SID and the benefits of irrigation.

The stored water is used to irrigate the lower parts of lowland rice fields (Fig. 1) by PIR from July 1 to 15, and the upper parts of lowland fields for soybean (as candidate crop for dry season cropping) by SID four times from December to February. Water balance was calculated under three cases of water management in the reservoirs as follows (Fig. 3): In Case 1, stored water was drained in early April (i.e., conventional use). In Case 2, stored water was drained in February when the 4^{th} SID was conducted while maintaining aquaculture. In Case 3, there was no aquaculture, and all stored water was used for irrigation. Finally, potential irrigation areas for PIR and SID were calculated under three water management scenarios. In Cases 1 and 2 where the minimum water level (water depth of 50 cm) for fish survival was constantly maintained, the results showed that potential irrigation area for PIR was 10.40 ha. In Case 3 where there was no aquaculture, it was 10.95 ha (Table 1). PIR enabled on-time transplanting in about 75% of lowland rice fields in the lower parts (14.1 ha). The potential irrigation areas for SID were 3.17, 3.37, and 3.52 ha in Cases 1, 2 and 3, respectively (Table 1). To calculate the benefits from irrigation, the incomes from the increase in rice and soybean yields due to irrigation and aquaculture, and aquaculture expenditures such as feed costs and compensation paid for losses due to the shortened period in Case 2 and compensation costs for excluding aquaculture in Case 3, were considered. The results showed that revenue growth can be expected from current state (i.e., no irrigation practice) in all Cases (Table 1). From the aspect of securing animal protein resources, it is desirable to maintain aquaculture (Cases 1 and 2).

The results of this research can be applied to other villages where rainy season lowland rice cultivation and aquaculture have been conducted as well as in N Village. However, potential irrigation areas should be calculated according to each village's own water resource and land use. In addition, in case power pumps or siphons are needed to withdraw water from reservoirs, costs related to equipment purchases and fuel should be included in the calculations.

(T. Anzai, H. Ikeura, A. Chomxaythong [National University of Laos (NUOL)], K. Keokhamphui [NUOL], S. Inkhamseng [NUOL], H. Fujimaki [Tottori University])

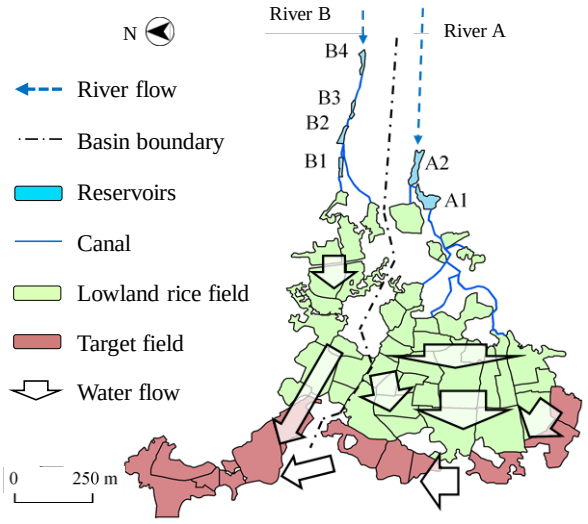

Fig. 1. Overview of river basins A and B in N Village

Note: Transplanting of rainy season lowland rice in the lower parts of lowland rice fields (shown as target field = 14.1 ha) was delayed due to water shortage in the early rainy season.

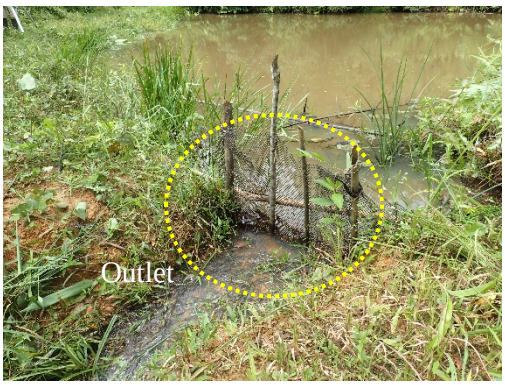

Fig. 2. Situation at the reservoir (B2)

Note 1: All reservoirs were constructed for aquaculture.

Note 2: Since the outlets were constructed at a high position in the dam body, a large portion of stored water has remained.

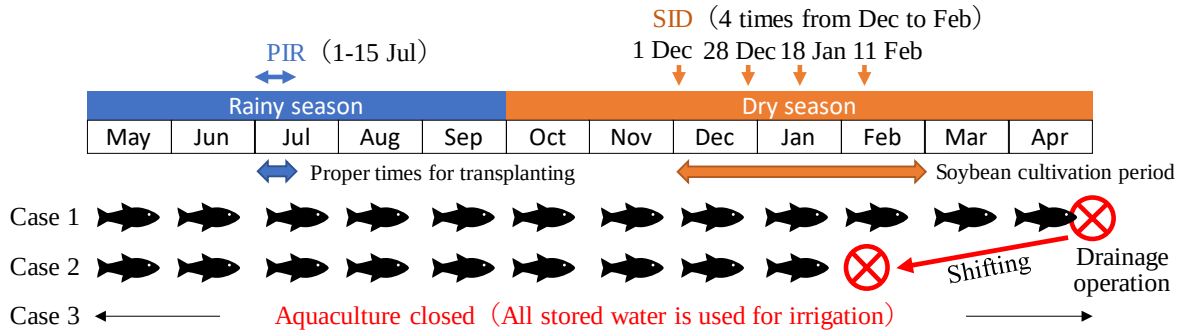

Fig. 3. Water management utilizing the reservoirs constructed for aquaculture

Note 1: In Cases 1 and 2, minimum water level (50 cm) is maintained for fish survival.

Note 2: In Case 1, stored water in the reservoirs is drained using water pump in April (conventional method).

Note 3: In Case 2, stored water in the reservoirs is drained to coincide with the 4th SID.

Table 1. Potential irrigation areas and preliminary calculations of projected increases in gross incomes (from current levels) due to irrigation practices

Water management	Potential irrigation area (ha)		Rice		Soybean production (ton) d (b×1.4 ton ha^{-1})	Benefits from irrigation (1,000 KIP)		
	PIR (a)	SID (b)	Yield (ton ha^{-1})	Increase in production (ton) c (a×(3.9-2.2) ton ha^{-1})		Total income (e) (c×2,500 KIP kg^{-1} +d×8,000 KIP kg^{-1})	Compensation cost f	Net income e-f
Current	No irrigation		2.2	0	0	-	-	0
Case 1	10.40	3.17	3.9	17.68	4.44	79,704	0	79,704
Case 2	10.40	3.37	3.9	17.68	4.72	81,944	720	81,224
Case 3	10.95	3.52	3.9	18.62	4.92	85,850	6,108	79,742

Note 1: As referred to in the study by Ikeura et al. (2016), the yield of rainy season lowland rice increases from 2.2 ton ha^{-1} to 3.9 ton ha^{-1} due to on-time transplanting through PIR.

Note 2: The average yield of soybean due to SID is assumed to be 1.4 ton ha^{-1}.

Note 3: In Case 2, reservoir owners are compensated with feeding fees. In Case 3, gross income from aquaculture is paid to reservoir owners as “loss of income compensation” .